NASA TN D-1815

NASA TN D-1815

TECHNICAL NOTE

D-1815

INVESTIGATION OF A SEMISPAN TILTING-PROPELLER CONFIGURATION AND EFFECTS OF RATIO OF WING CHORD TO PROPELLER DIAMETER ON SEVERAL SMALL-CHORD TILTING-WING CONFIGURATIONS AT TRANSITION SPEEDS

By Kenneth P. Spreemann

Langley Research Center
Langley Station, Hampton, Va.

NATIONAL AERONAUTICS AND SPACE ADMINISTRATION
WASHINGTON
July 1963

NATIONAL AERONAUTICS AND SPACE ADMINISTRATION

TECHNICAL NOTE D-1815

INVESTIGATION OF A SEMISPAN TILTING-PROPELLER CONFIGURATION AND EFFECTS OF RATIO OF WING CHORD TO PROPELLER DIAMETER ON SEVERAL SMALL-CHORD TILTING-WING CONFIGURATIONS AT TRANSITION SPEEDS

By Kenneth P. Spreemann

SUMMARY

An investigation of the effects of changes in the ratio of wing chord to propeller diameter of three tilting-wing and tilting-propeller VTOL models has been conducted in the 17-foot test section of the Langley 300-MPH 7- by 10-foot tunnel. The models had wing-chord—propeller-diameter ratios of 0.333, 0.208, and 0.125 with a single propeller 2.00 feet in diameter located at the wing tips.

The investigation indicated that reductions in the ratio of wing chord to propeller diameter made small changes in lift, drag, and pitching moment; this indicates that with the small ratios of wing chord to propeller diameter in this investigation these configurations would realize small aerodynamic forces and moments in comparison with those realized from direct propeller thrust.

The data are used in an analysis in which a full-scale aircraft is assumed to be in steady level flight. All the tilting-wing configurations investigated were generally stalled throughout most of the level-flight transition speed range. The power required in level-flight transition did not exceed that required for hovering on any of the configurations investigated. The stall would probably make these basic configurations unacceptable, however, from the point of view of handling qualities.

The power required by the tilting propeller in transition was as high as the most severely stalled tilting wing and was considerably above that required for an unstalled tilting wing from a previous investigation; this high power requirement thus indicates relatively poor STOL performance.

INTRODUCTION

Many methods of obtaining satisfactory vertical take-off and landing (VTOL) and short take-off and landing (STOL) flight have been proposed and investigated.

Two configurations capable of realizing VTOL flight and STOL flight, the tilting wing and the tilting propeller, are studied in this investigation.

A previous investigation (ref. 1) indicated that for tilting-wing configurations the stall in the transition speed range is a major factor affecting the power requirements. Presented in reference 1 are data for large wing-chord—propeller-diameter ratios for a tilting-wing configuration.

The present investigation is intended to extend the scope of reference 1 to much smaller ratios of wing chord to propeller diameter in order to determine the limiting values, if any, on the stalling characteristics in transition. The effects of direction of propeller rotation were also investigated. In addition, a comparison with a tilting-propeller configuration is presented.

COEFFICIENTS AND SYMBOLS

The force and moment coefficients used in this paper are based on the calculated dynamic pressure in the slipstream. The positive sense of forces, moments, and angles is indicated in figure 1. The pitching moments are referred to the wing quarter-chord point.

$C_{L,s}$ lift coefficient, $\frac{L}{q_s S}$

$C_{X,s}$ longitudinal-force coefficient, $\frac{F_X}{q_s S}$

$C_{m,s}$ pitching-moment coefficient, $\frac{M_Y}{q_s S c}$

$C_{T,s}$ thrust coefficient, $\frac{T_p}{q_s \frac{\pi D^2}{4}}$

D model propeller diameter, ft

F_X longitudinal force, Thrust $\times \cos \alpha_{T.L.}$ - Drag, lb

P_{req} power required of assumed airplane, hp

L lift of model, lb

M_Y pitching moment of model, ft-lb

$M_{Y,a}$ pitching moment of airplane, ft-lb

S wing area of semispan model, sq ft

T_p propeller thrust, lb

V free-stream velocity, ft/sec

V_a airplane velocity, knots

c wing chord, ft

q free-stream dynamic pressure, $\frac{1}{2}\rho V^2$, lb/sq ft

q_s slipstream dynamic pressure, $q + \frac{T_p}{\pi D^2/4}$, lb/sq ft

$\alpha_{T.L.}$ angle of attack of thrust line, deg

α_w wing angle of attack, deg

i_p propeller center-line incidence with reference to wing-chord plane, deg

ρ mass density of air in free stream, slug/cu ft

δ_f flap deflection with respect to wing-chord plane, deg

MODELS AND APPARATUS

A drawing of the three basic configurations with pertinent dimensions are given in figure 2. The geometric characteristics of the semispan models are given in the following table:

Chord, ft	c/D	Area, sq ft	Aspect ratio	Airfoil section
0.667	0.333	1.028	4.62	NACA 4415
.417	.208	.642	7.39	NACA 4415
.250	.125	.385	12.31	NACA 4424

The semispan models had a single propeller 2.00 feet in diameter located at the wing tip. One propeller rotating with the wing-tip vortex and one propeller rotating against the wing-tip vortex were tested in order to assess the effects of direction of propeller rotation. The wing with $c/D = 0.333$ was equipped with a single slotted flap as shown in figure 3. The wing with $c/D = 0.208$ was

constructed so that the propeller could be tilted with respect to the wing-chord plane from 0° to 90°.

The motor was mounted inside a nacelle by means of strain-gage balances so that thrust and torque of the propeller could be measured. The total model lift, longitudinal force, and pitching moment were measured by a strain-gage balance mounted beneath the tunnel floor.

TESTS AND CORRECTIONS

The tests were conducted in the 17-foot test section of the Langley 300-MPH 7- by 10-foot tunnel. The arrangement and calibration of this test section are given in the appendix of reference 2. Combinations of free-stream dynamic pressures and propeller thrusts were selected to maintain a dynamic pressure of approximately 8 pounds per square foot in the propeller slipstream. The model thrust coefficient was varied by changing the propeller thrust and the tunnel dynamic pressure. Once a particular test condition was established the propeller thrust was held approximately constant throughout the angle-of-attack range.

Corrections to the free-stream velocity to account for blockage and slipstream contraction were estimated and found to be negligible and, thus, were not considered. The jet-boundary corrections were estimated for a square test section by a method similar to that of reference 3 and, although small, were applied to the angle of attack and the longitudinal force. The tests were run at Reynolds numbers, based on wing chord and average slipstream velocity, of 131,000 for the 3-inch-chord wing, 218,000 for the 5-inch-chord wing, and 350,000 for the 8-inch-chord wing.

PRESENTATION OF RESULTS

The results of the investigation are presented in the following figures:

For summary figures 10 to 13, the model was treated as a 0.167-scale model of a 10,000-pound airplane; the model and full-scale coefficients were arbitrarily assumed to be equal. The propeller performance was calculated from data for propeller 1 of reference 4 for all configurations except the tilting-propeller configuration (first two configurations in fig. 13) for which data for propeller 2 were utilized.

DISCUSSION

Effect of c/D and Wing Span

The basic data given in figures 4, 5, and 6 show that all the wings of this investigation were generally stalled in steady level flight ($C_{X,s} = 0$) at the higher transition speeds, lower $C_{T,s}$ range, regardless of whether or not the flaps were deflected. Also, the stall extends well into the climb region at these speeds.

The nondimensional data of figures 4(a), 5(a), and 6 show an increase in the value of the coefficients as the wing-chord—propeller-diameter ratio is reduced. In actuality the lift, drag, and pitching moment change little with change in chord-diameter ratio. The change in coefficient is due to the change in reference area used, indicating that with the range of wing-chord—propeller-diameter ratios and low speeds employed in this investigation the direct propeller thrust components were the primary contributors to the forces and moments. This is shown in the summary data presented in figure 10 where the steady-level-flight characteristics are presented for an assumed 10,000-pound airplane; similar results are generally shown for all wing-chord—propeller-diameter ratios.

It is interesting to note that even at the lowest chord-diameter ratios the power required in transition did not exceed that required in hovering as was feared might occur (ref. 1).

The effects of increasing the wing span and chord are shown in figure 11 for the assumed 10,000-pound airplane. The short-span-wing basic data are from figure 4 of this paper and the data for the other configurations are from reference 1.

Increasing the wing span had little effect on power required. Increasing the chord and adding a leading-edge slat provided a large reduction in power required. The large-chord configuration with slat was nearly free from stall and is used herein to indicate the characteristics that can be obtained with an unstalled wing. The reduction in power required in transition is important from

the point of view of both safety and STOL performance (ref. 5). Also, the reduced angle of attack in transition would greatly reduce the propeller loads and vibrations.

The large-chord tilting wing (c/D = 0.75) of reference 1 is used herein to illustrate these points because it is most directly comparable. Both references 2 and 5 show, however, that a flapped tilting-wing configuration is much more desirable. Improved stall control is obtained and the destabilizing moments from the propeller, see top of figure 12, can be countered by the diving moments of the flap (as shown in ref. 2).

From the basic data of figures 4, 5, 7, and 8, the effects of propeller rotation on power required and pitching moment were calculated for the assumed 10,000-pound airplane; the results are given in figure 12. Rotating the propeller against the tip vortex gave a slight reduction in power required in the transition speed range.

Comparison of Tilting-Wing and Tilting-Propeller Configurations

The variation of lift, longitudinal-force, and pitching-moment coefficients with thrust coefficient for the tilting-propeller configuration at wing angles of attack of 0° and 10° are given in figure 9. The related power, propeller incidence, and pitching-moment variation with speed in transition for the assumed 10,000-pound airplane are shown in figure 13. It is seen that tilting the propeller only as compared with tilting the wing and propeller together had little effect on the power required in the low transition speed range. Raising the wing angle of attack 10° with the tilting propeller provided a small reduction in power required because of the increased aerodynamic lift. The power required by the tilting propeller in transition was considerably higher than that required for the unstalled tilting wing of reference 1; this indicates relatively poor STOL performance.

Although the differences between the tilting-wing and the tilting-propeller configurations at this particular chord-diameter ratio as far as power required is concerned were not great, there could be very significant differences from the flying qualities point of view. This small-chord tilting wing is severely stalled throughout most of the transition speed range and would very likely experience serious buffet, whereas the tilting propeller at these wing angles of attack is unstalled. A tilting-wing configuration, however, can be fixed to minimize the stall as indicated in references 1 and 2, and as shown in figure 13 the power required for the largest chord wing with leading-edge slat is considerably less than that of the tilting-propeller configuration.

The greater power required by the tilting propeller in hovering is due to the wing being normal to the slipstream and thus experiencing a down load. This point is illustrated in figures 5(a) and 5(g). At $C_{T,s} = 1.0$ in figure 5(a), $C_{L,s} \approx 5.0$ for what would be the tilting-wing configuration, but in figure 5(g) $C_{L,s} \approx 4.5$ for the tilting-propeller configuration. Additional data on these effects are contained in reference 6.

CONCLUSIONS

An investigation of the effects of changes in the ratio of wing chord to propeller diameter of three tilting-wing and tilting-propeller VTOL models and an analysis in which a full-scale airplane was assumed to be in level flight indicated the following conclusions:

1. Reductions in the ratio of wing chord to propeller diameter resulted in only small changes in lift, drag, and pitching moment; this indicates that with the small wing-chord—propeller-diameter ratios in this investigation the direct propeller thrust components were the primary contributors to the aerodynamic forces and moments.

2. All the tilting-wing configurations investigated were generally stalled throughout most of the level-flight transition speed range.

3. The power required in level-flight transition did not exceed that required for hovering on any of the configurations investigated. The stall would probably make these basic configurations unacceptable, however, from the point of view of handling qualities.

4. The power required by the tilting propeller in transition was as high as the most severely stalled tilting wing and was considerably above that required for an unstalled tilting wing; this indicates relatively poor STOL performance.

Langley Research Center,
National Aeronautics and Space Administration,
Langley Station, Hampton, Va., May 2, 1963.

REFERENCES

1. Taylor, Robert T.: Wind-Tunnel Investigation of Effect of Ratio of Wing Chord to Propeller Diameter With Addition of Slats on the Aerodynamic Characteristics of Tilt-Wing VTOL Configurations in the Transition Speed Range. NASA TN D-17, 1959.

2. Kuhn, Richard E., and Hayes, William C., Jr.: Wind-Tunnel Investigation of Longitudinal Aerodynamic Characteristics of Three Propeller-Driven VTOL Configurations in the Transition Speed Range, Including Effects of Ground Proximity. NASA TN D-55, 1960.

3. Gillis, Clarence L., Polhamus, Edward C., and Gray, Joseph L., Jr.: Charts for Determining Jet-Boundary Corrections for Complete Models in 7- by 10-Foot Closed Rectangular Wind Tunnels. NACA WR L-123, 1945. (Formerly NACA ARR L5G31.)

4. Yaggy, Paul F., and Rogallo, Vernon L.: A Wind-Tunnel Investigation of Three Propellers Through an Angle-of-Attack Range From 0° to 85°. NASA TN D-318, 1960.

5. Kuhn, Richard E.: Review of Basic Principles of V/STOL Aerodynamics. NASA TN D-733, 1961.

6. McKee, John W., and Naeseth, Rodger L.: Experimental Investigation of the Drag of Flat Plates and Cylinders in the Slipstream of a Hovering Rotor. NACA TN 4239, 1958.

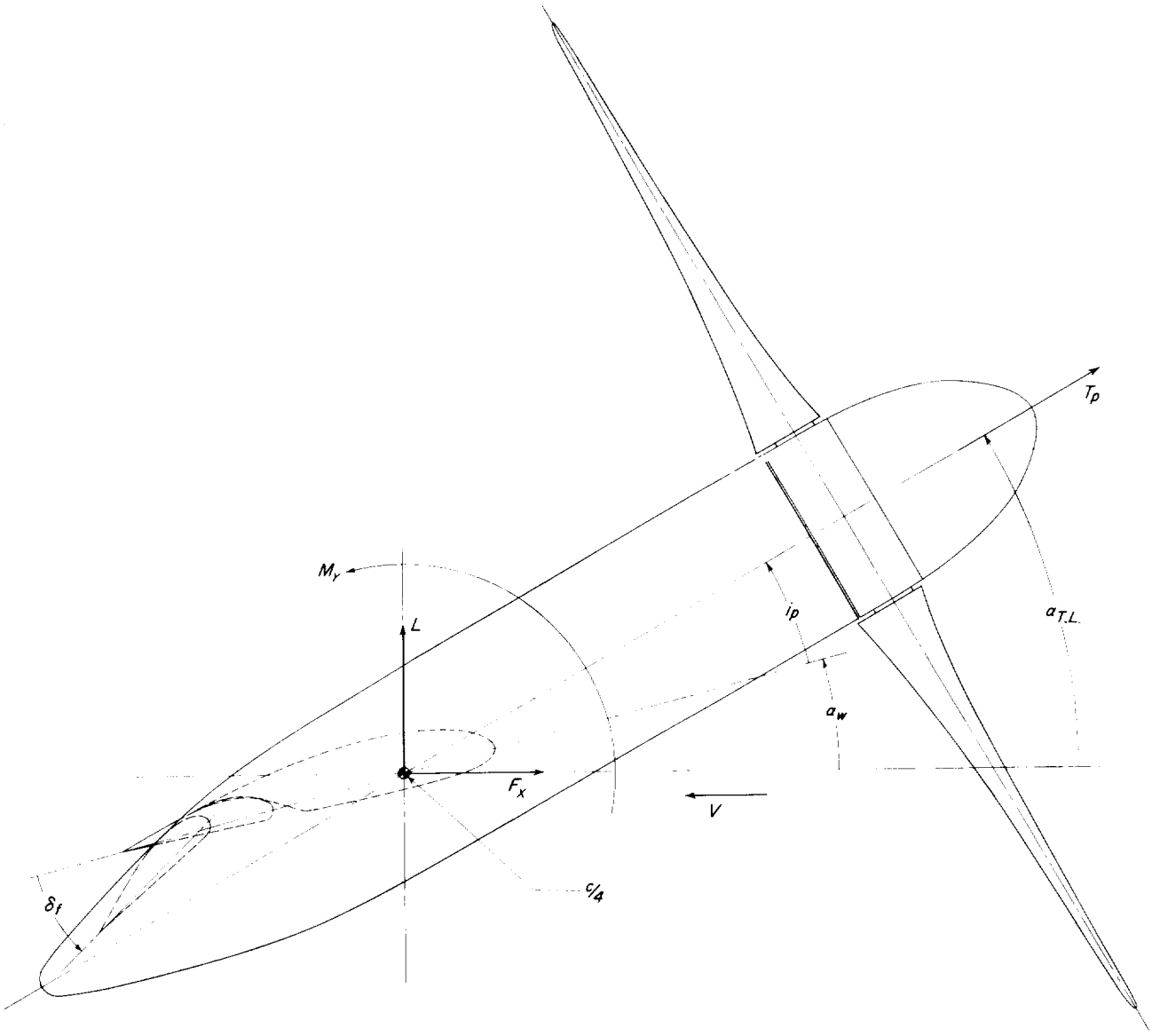

Figure 1.- Conventions used to define positive sense of forces, moments, and angles.

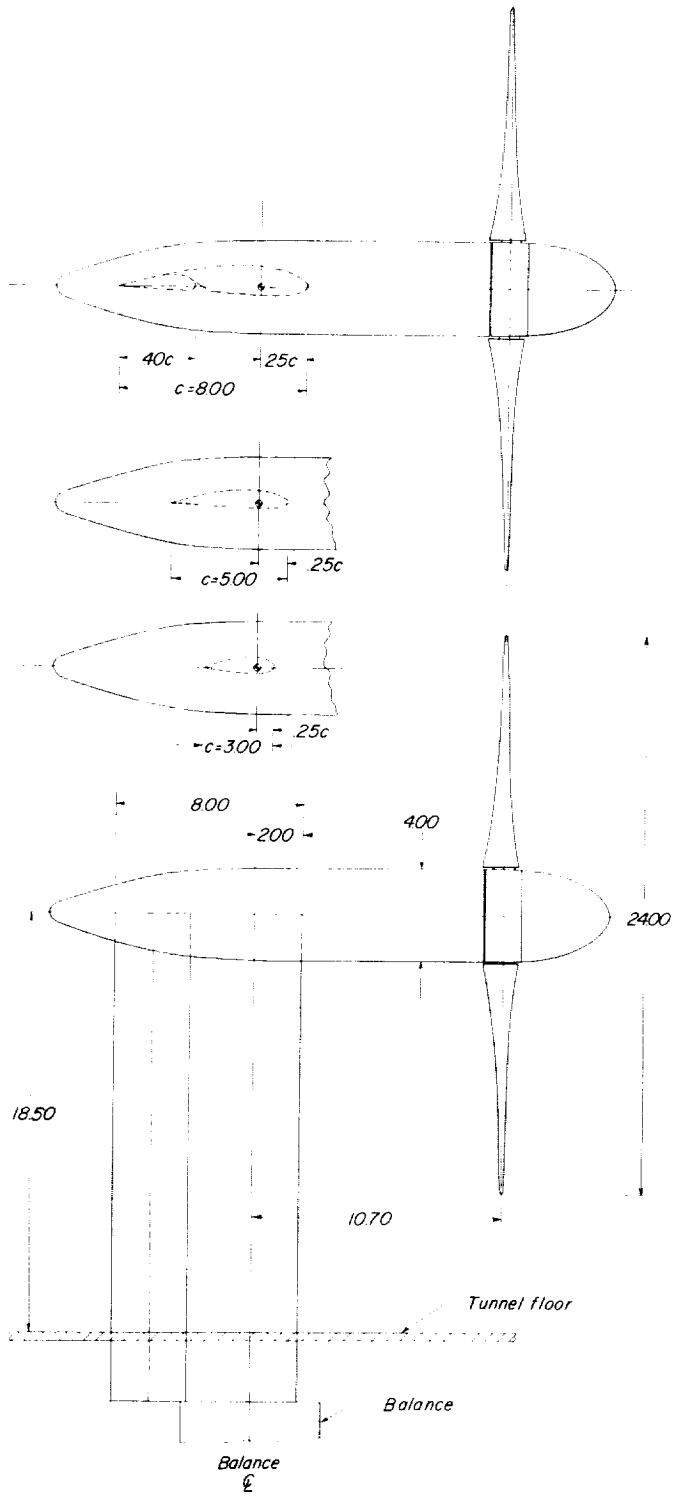

Figure 2.- Sketch of three configurations investigated. (All dimensions are in inches.)

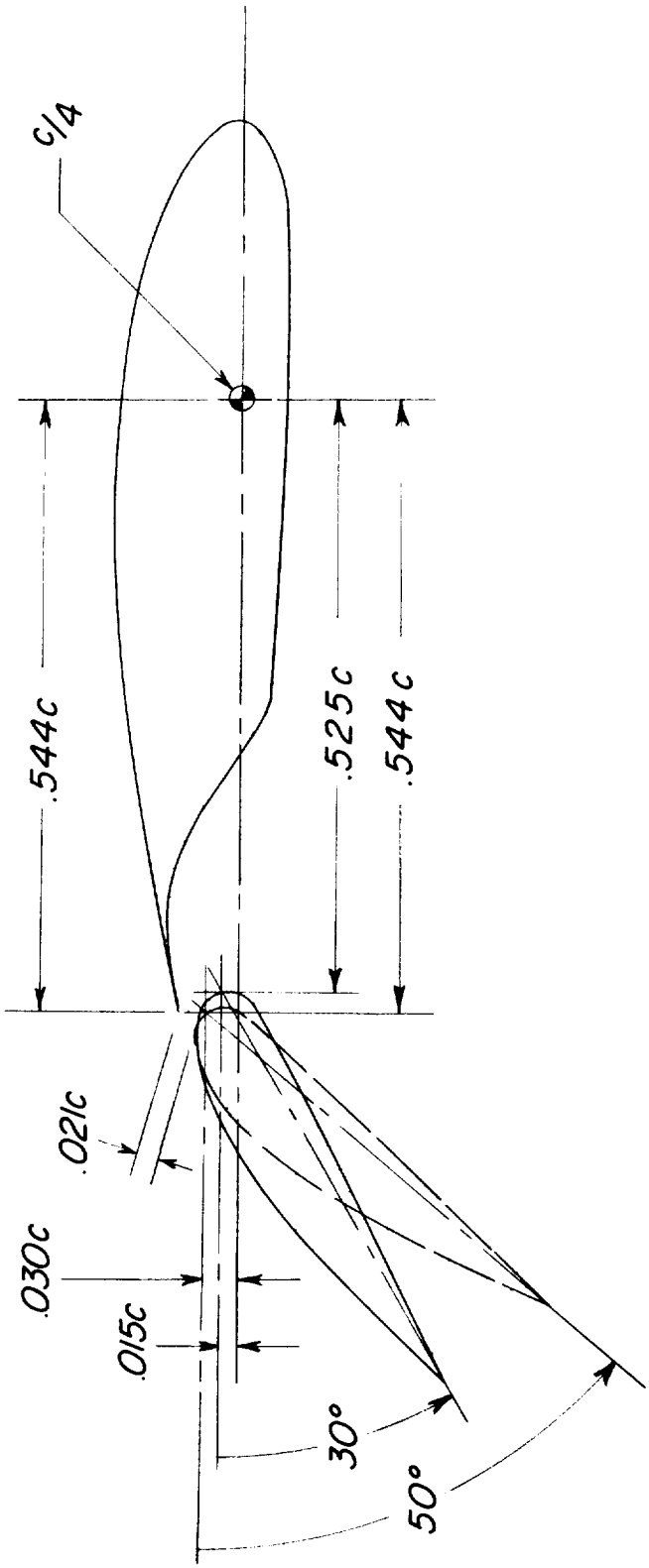

Figure 3.- Flap positions employed on the 8-inch-chord wing configuration.

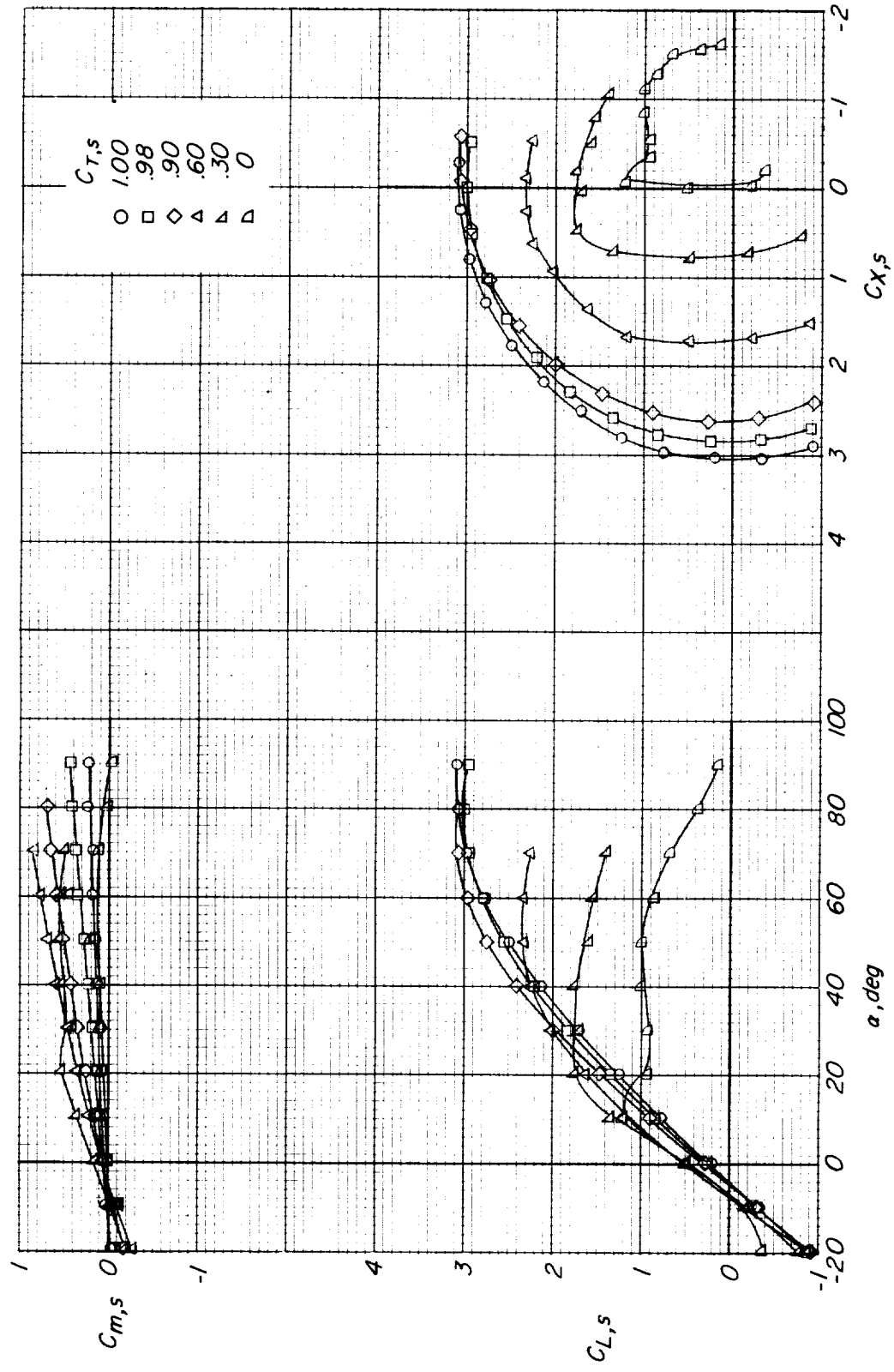

(a) $\delta_f = 0°$.

Figure 4.- Aerodynamic characteristics of tilting-wing configuration with c/D = 0.333 and propeller rotation against wing-tip vortex. $i_p = 0°$.

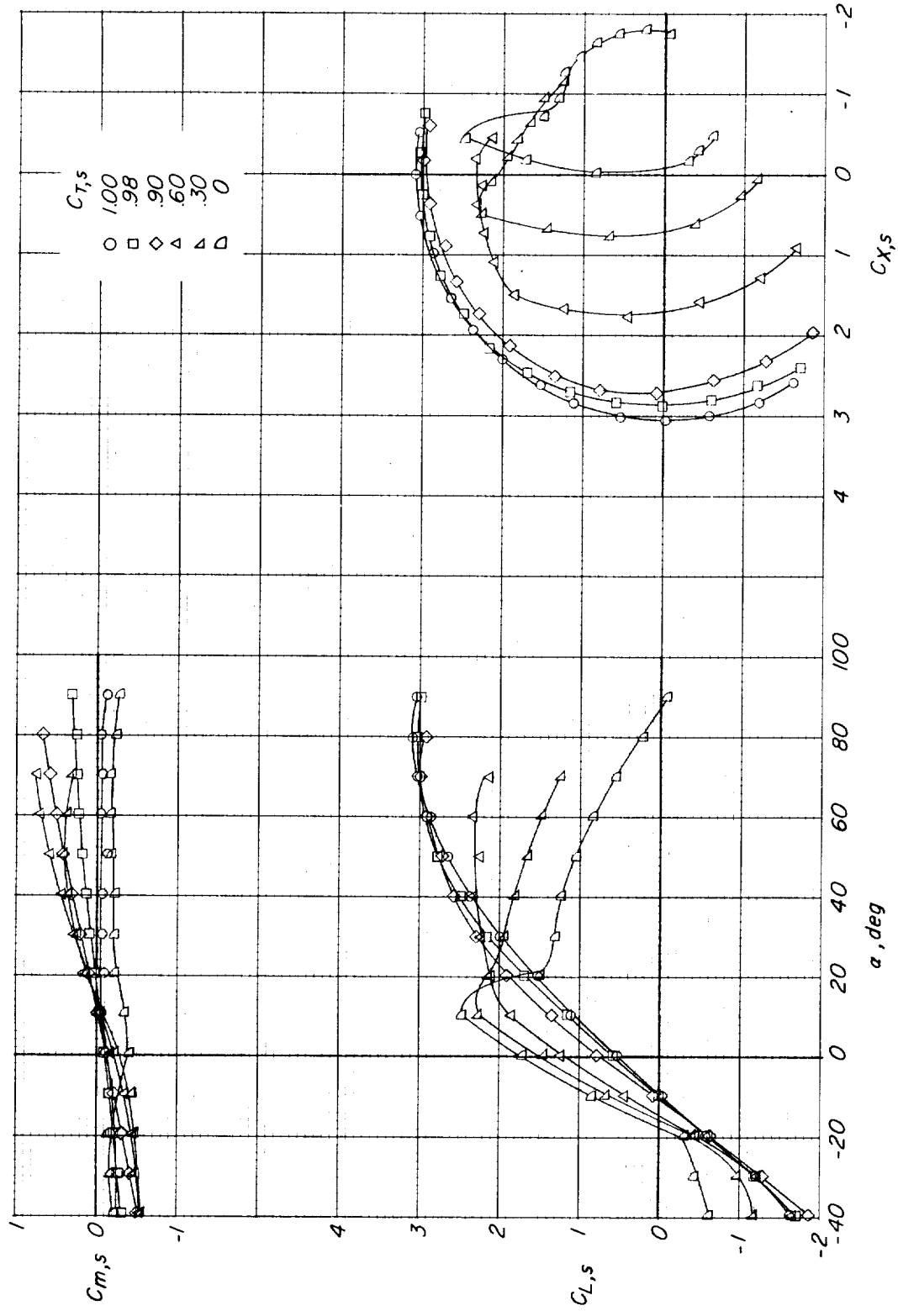

(b) $\delta_f = 30^\circ$.

Figure 4.- Continued.

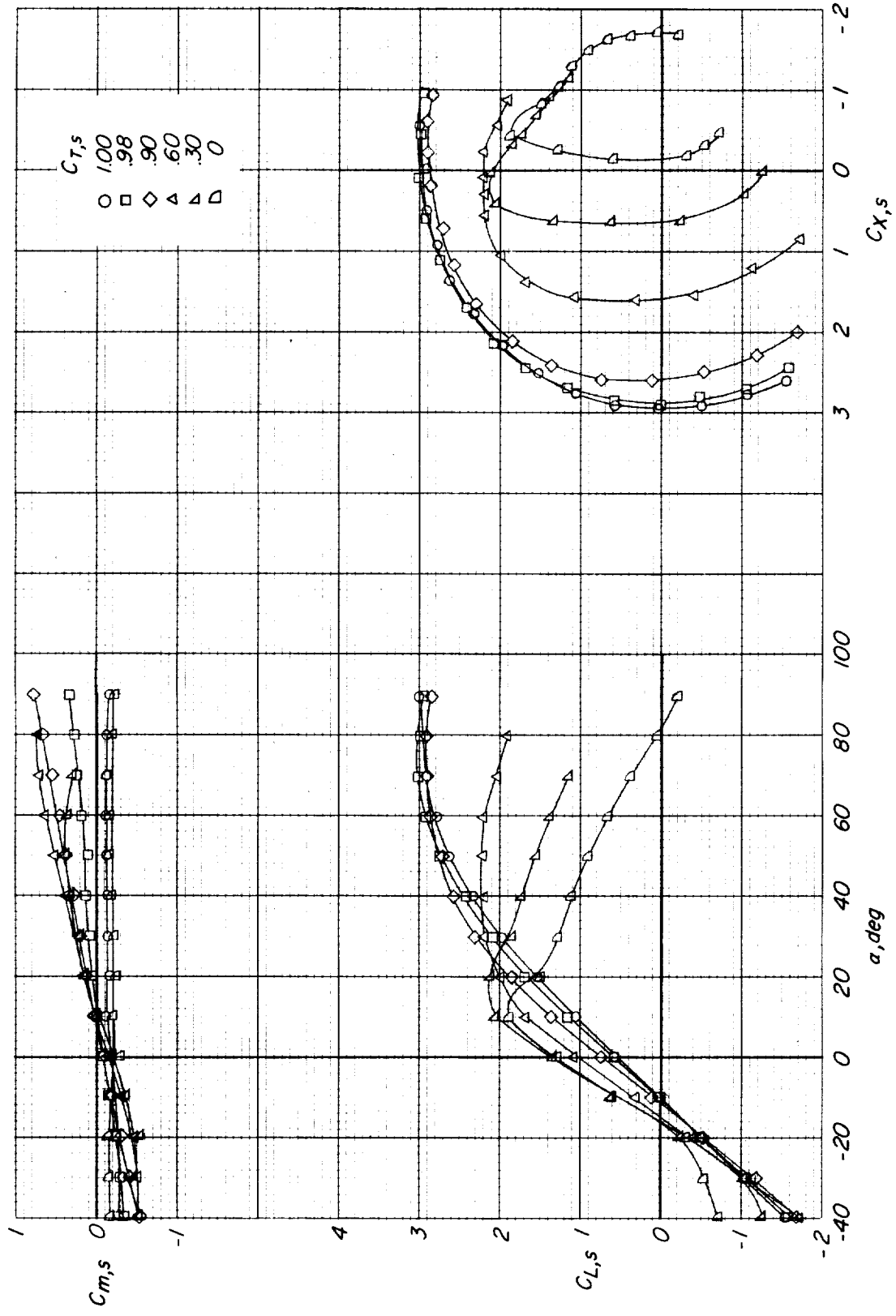

(c) $\delta_f = 50^\circ$.

Figure 4.- Concluded.

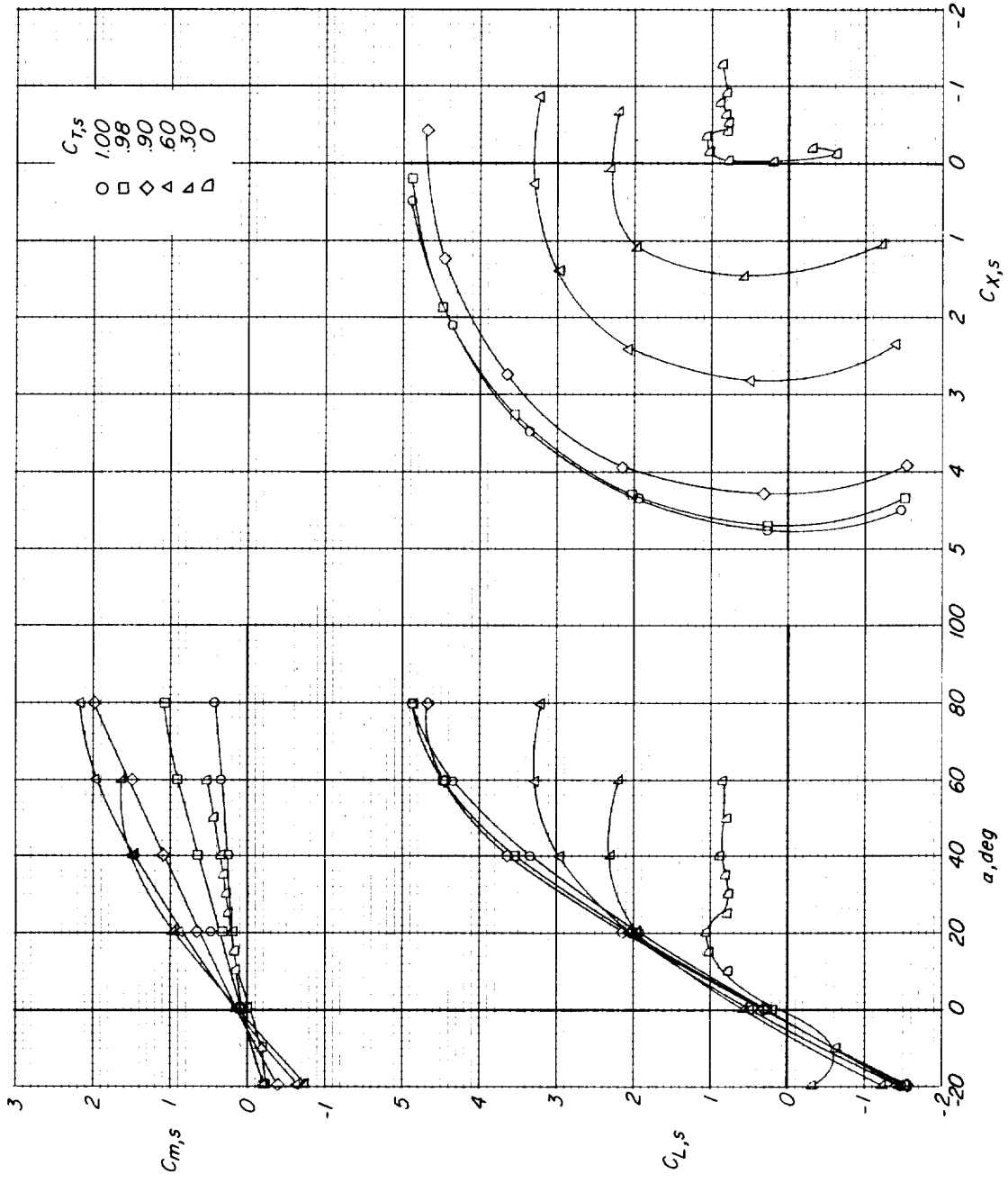

(a) $i_p = 0°$.

Figure 5.- Aerodynamic characteristics of tilting-propeller configuration with c/D = 0.208 and propeller rotation against wing-tip vortex. $\delta_f = 0°$.

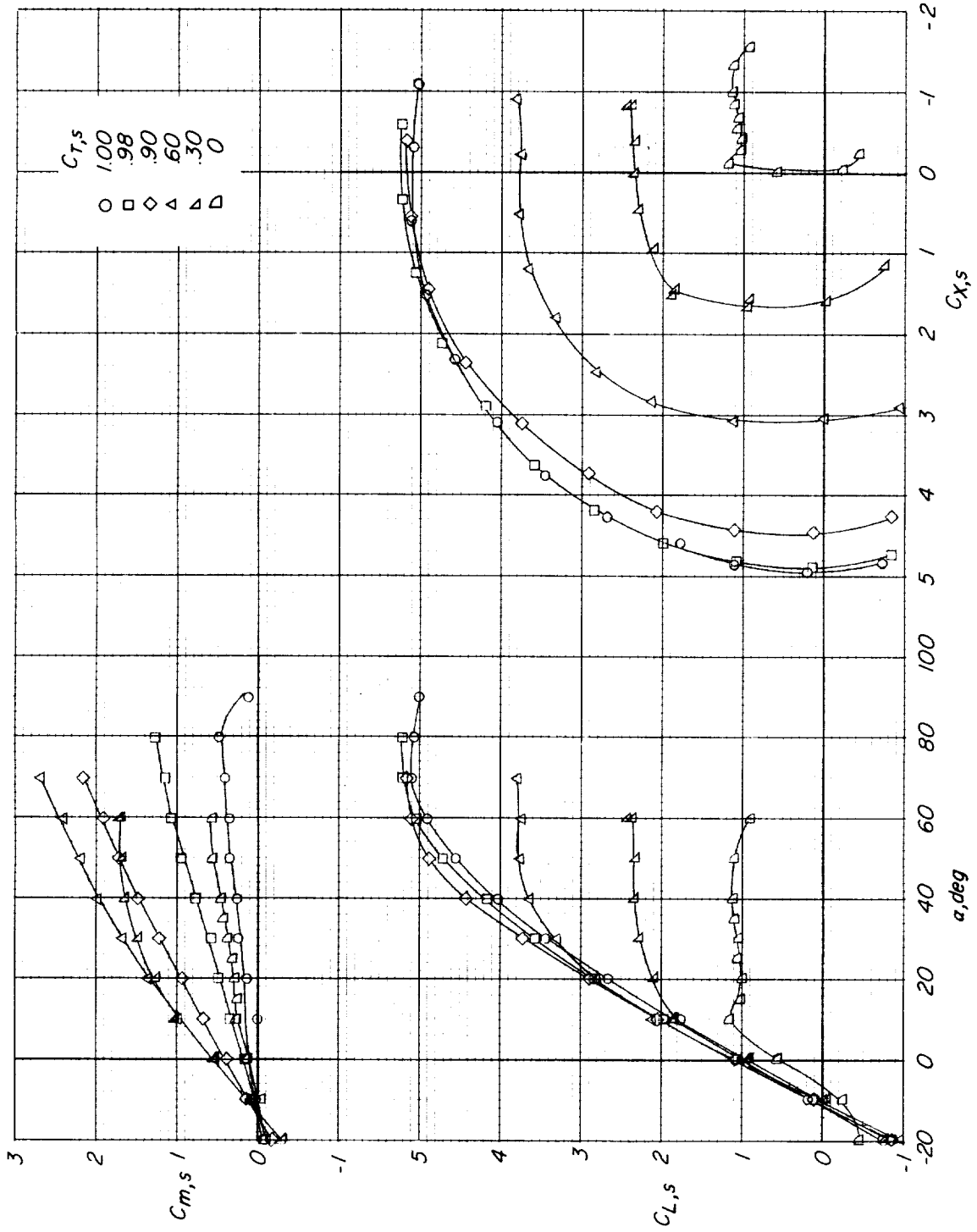

(b) $i_p = 10°$.

Figure 5.- Continued.

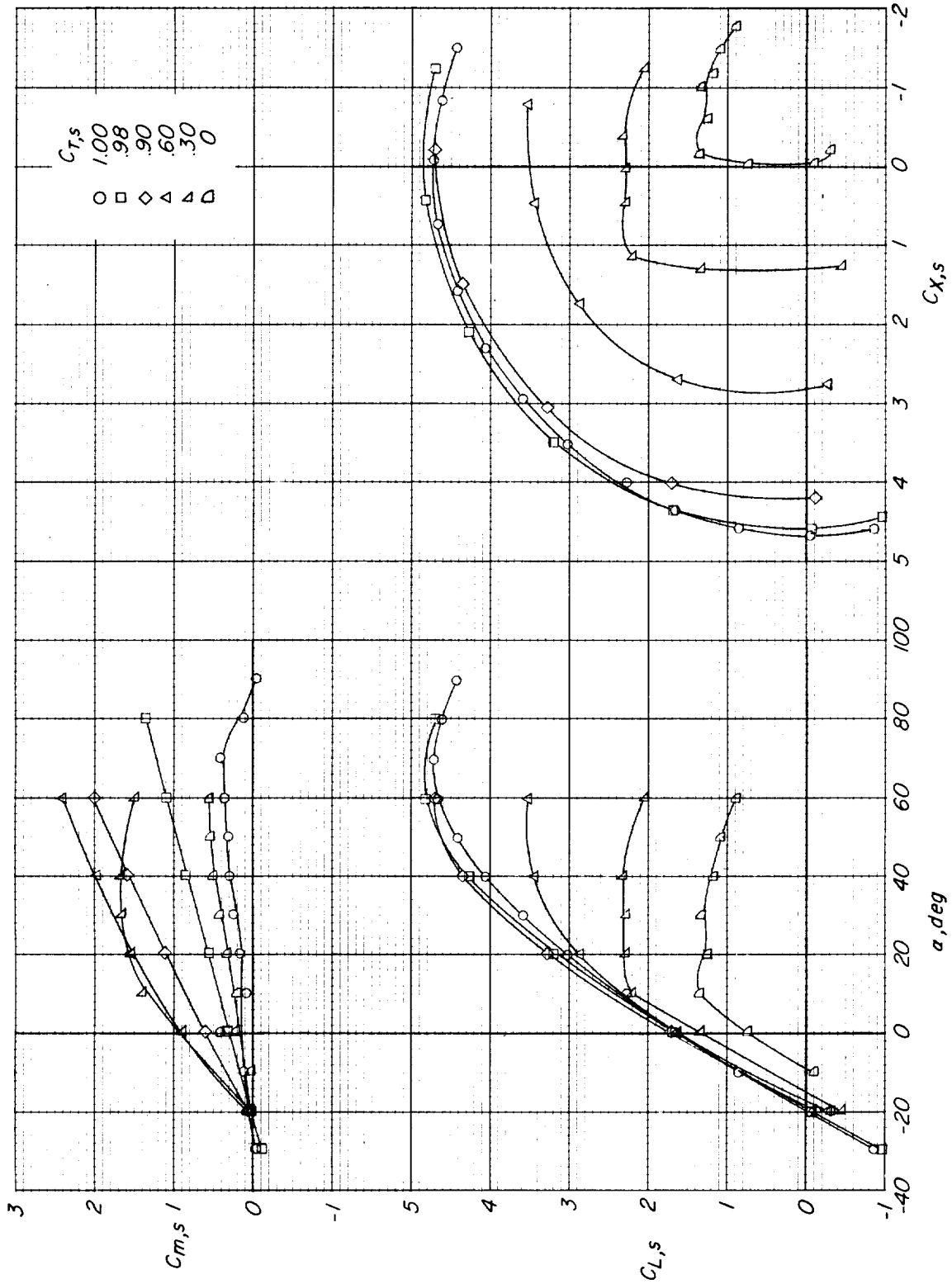

(c) $i_p = 20°$.

Figure 5.- Continued.

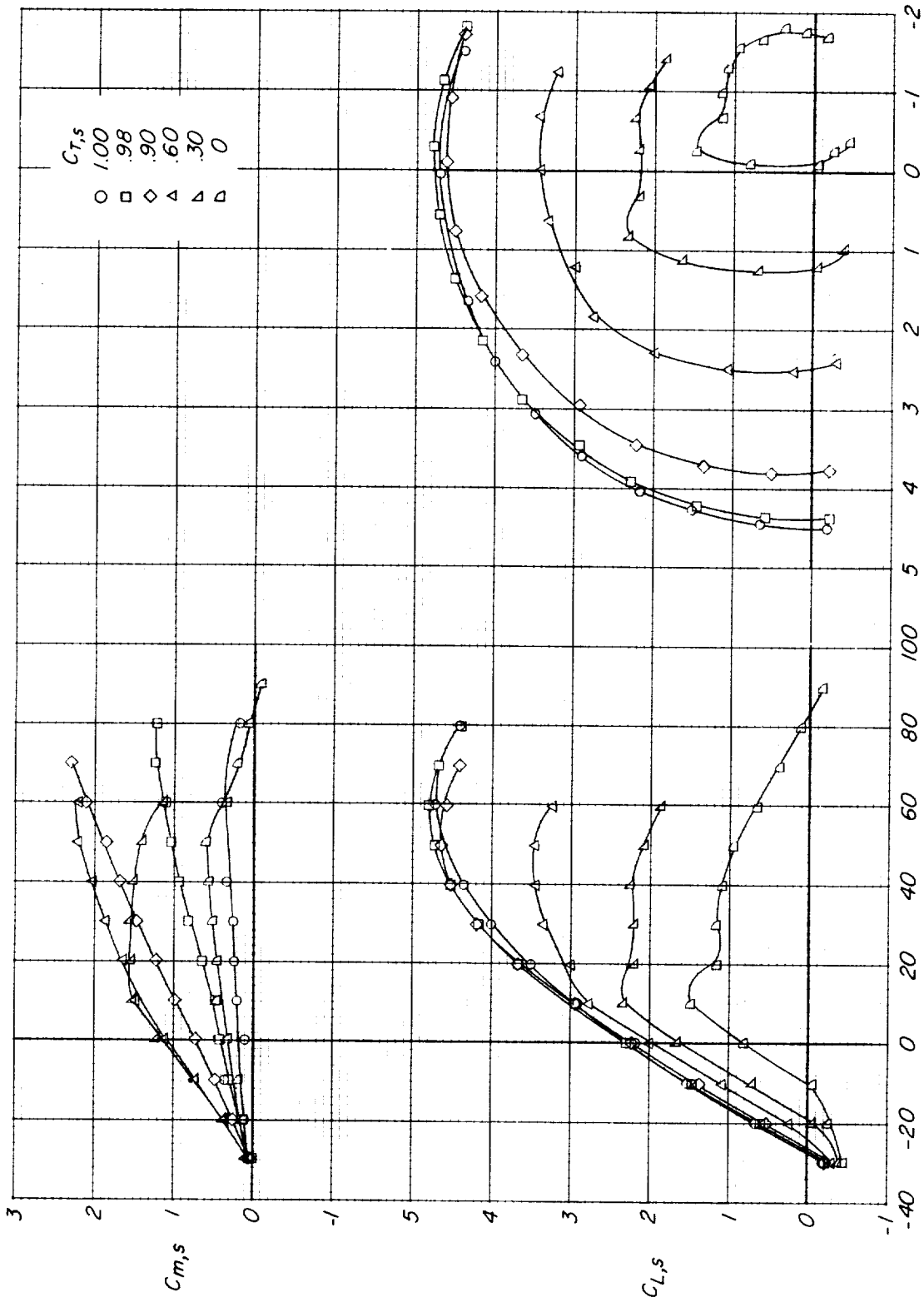

(d) $i_p = 30°$.

Figure 5.- Continued.

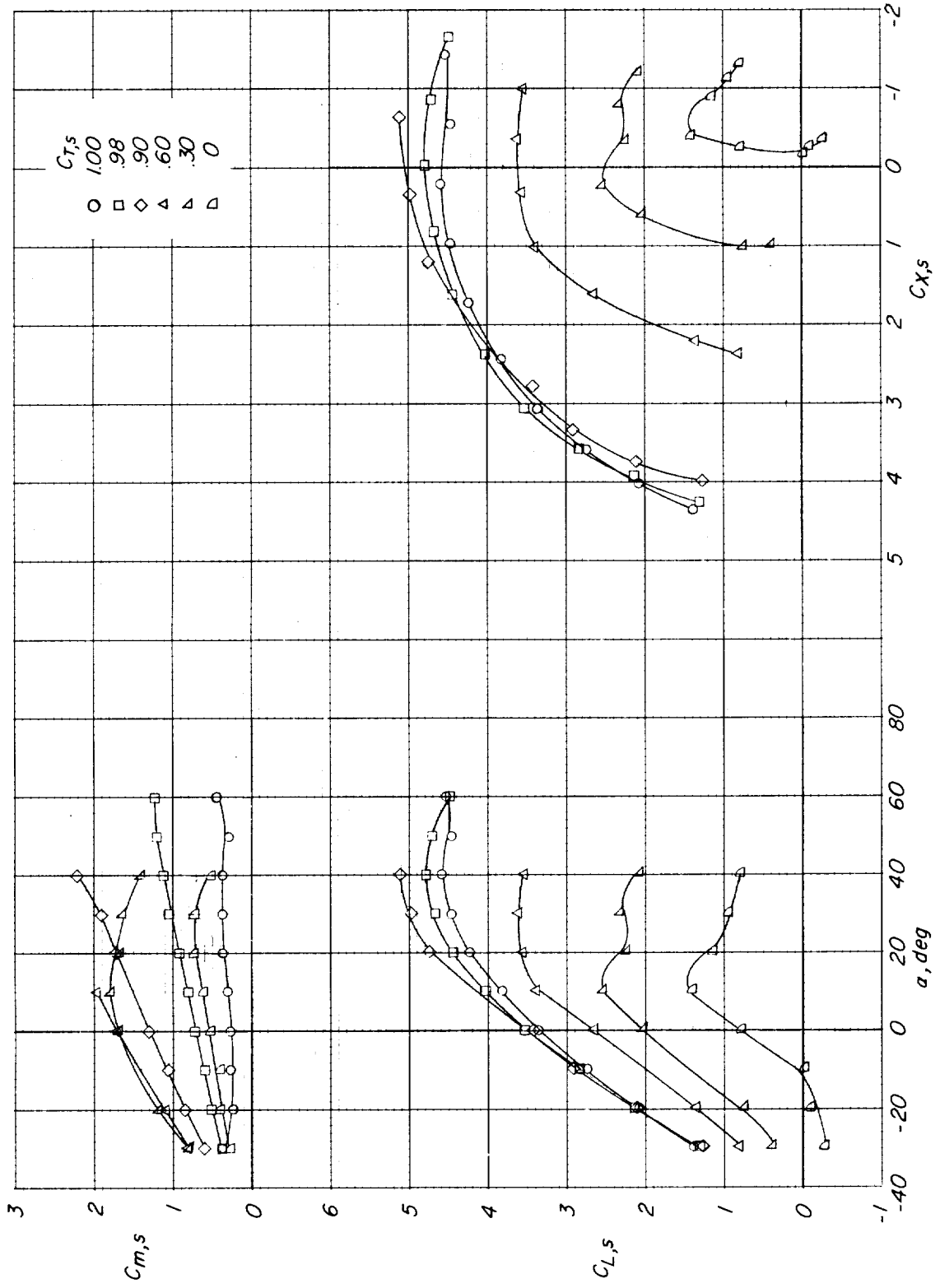

(e) $i_p = 50°$.

Figure 5.- Continued.

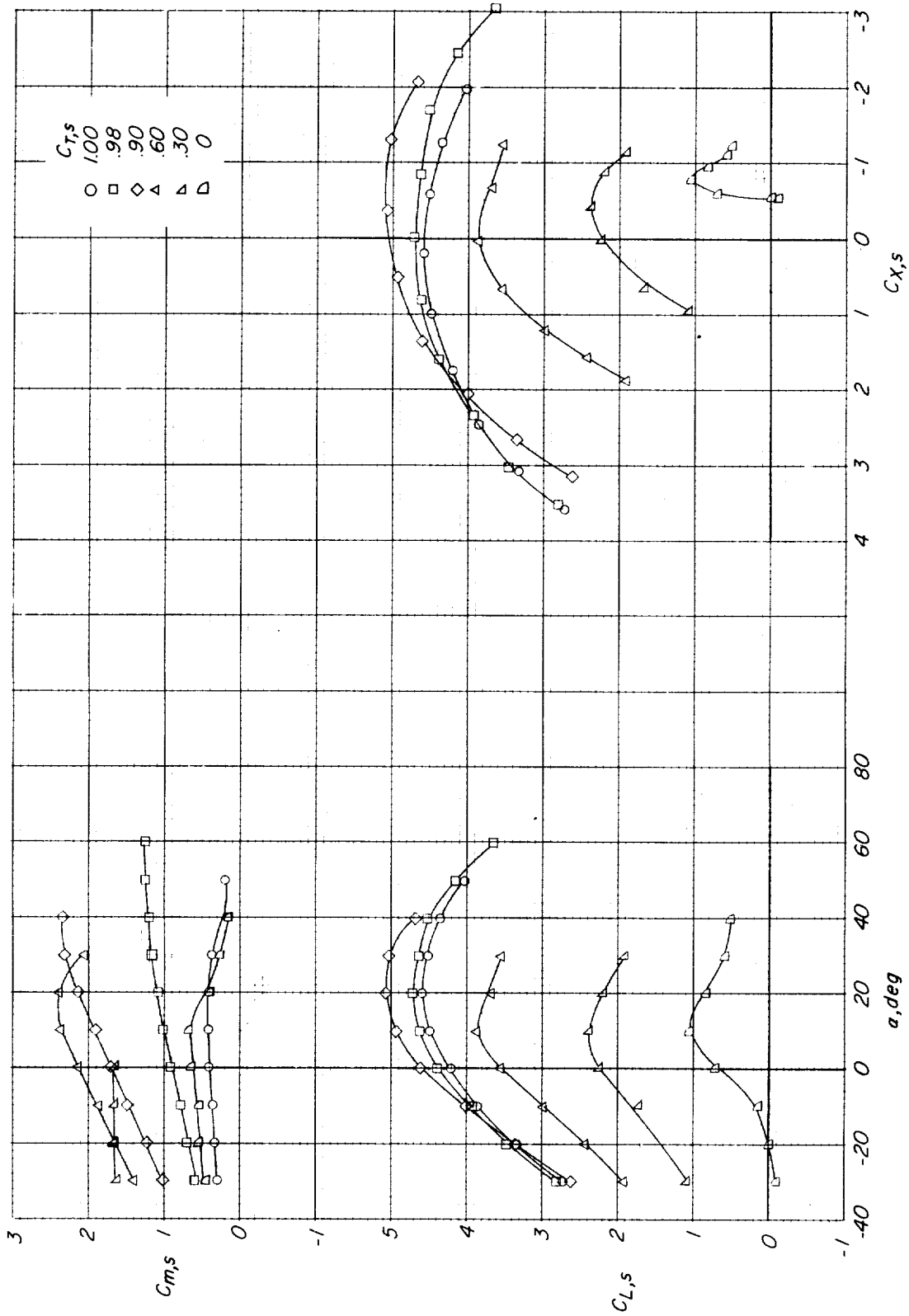

(f) $i_p = 70°$.

Figure 5.- Continued.

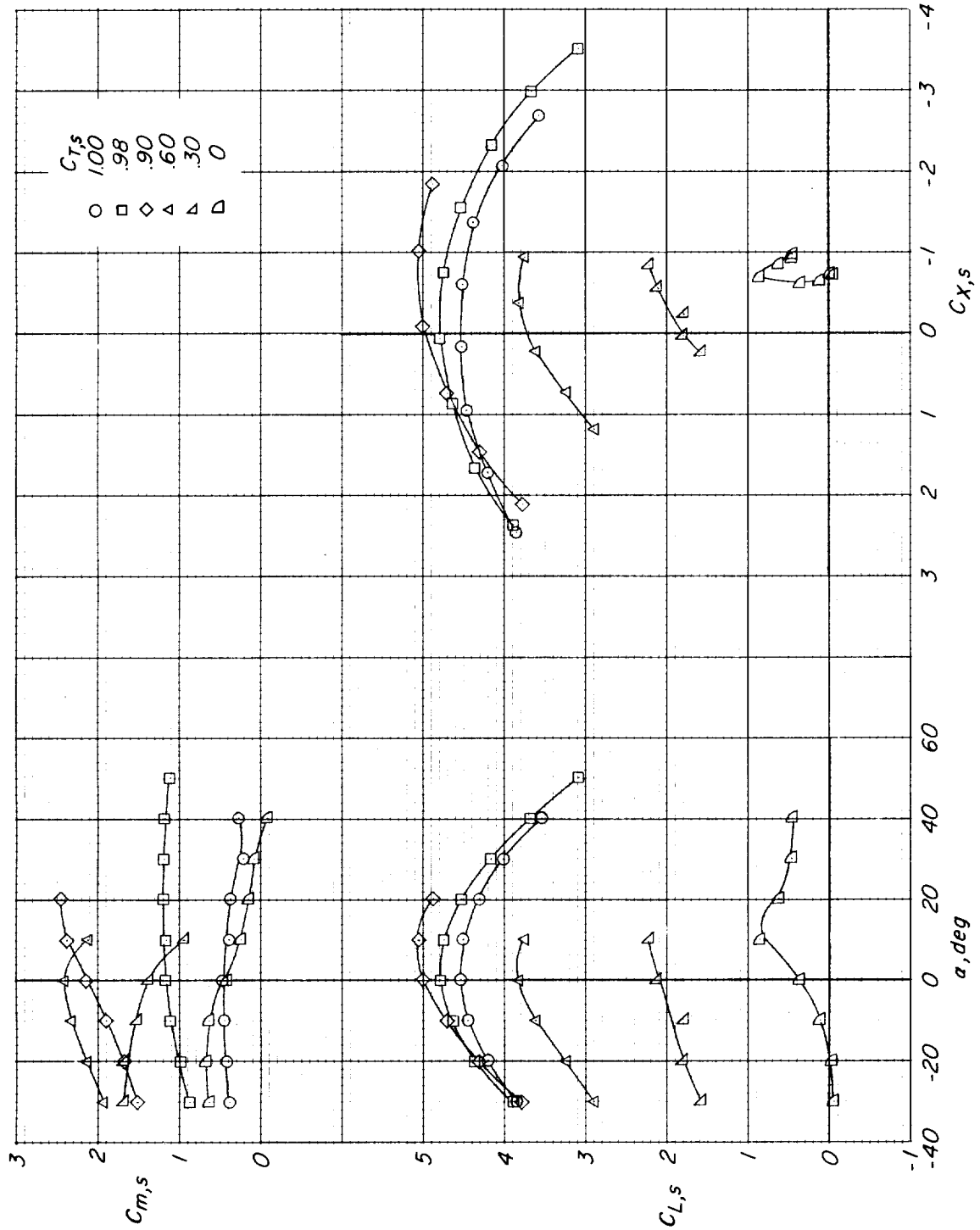

(g) $i_p = 90°$.

Figure 5.- Concluded.

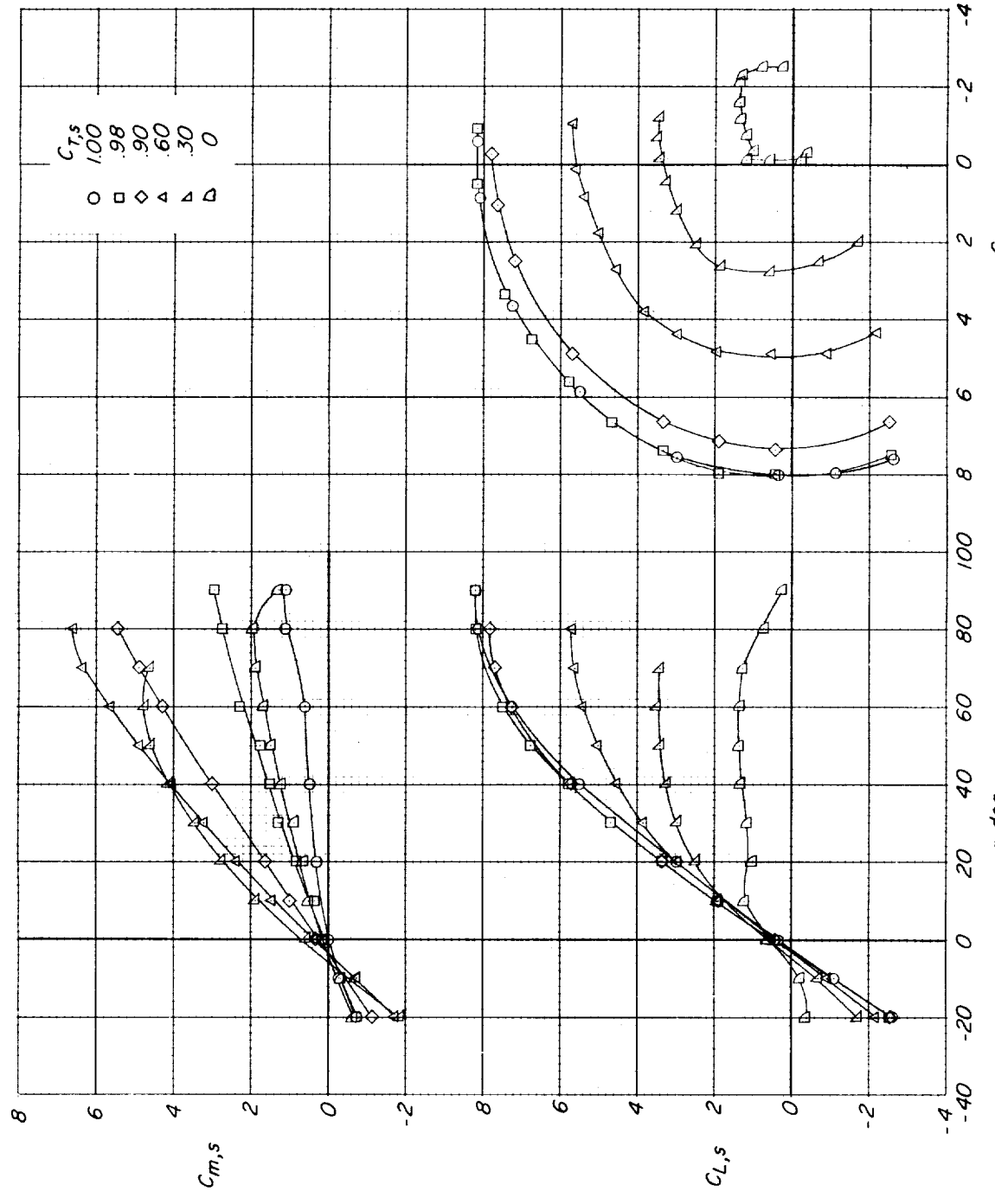

Figure 6.- Aerodynamic characteristics of tilting-wing configuration with c/D = 0.125 and propeller rotation against wing-tip vortex $i_p = 0°$; $\delta_f = 0°$.

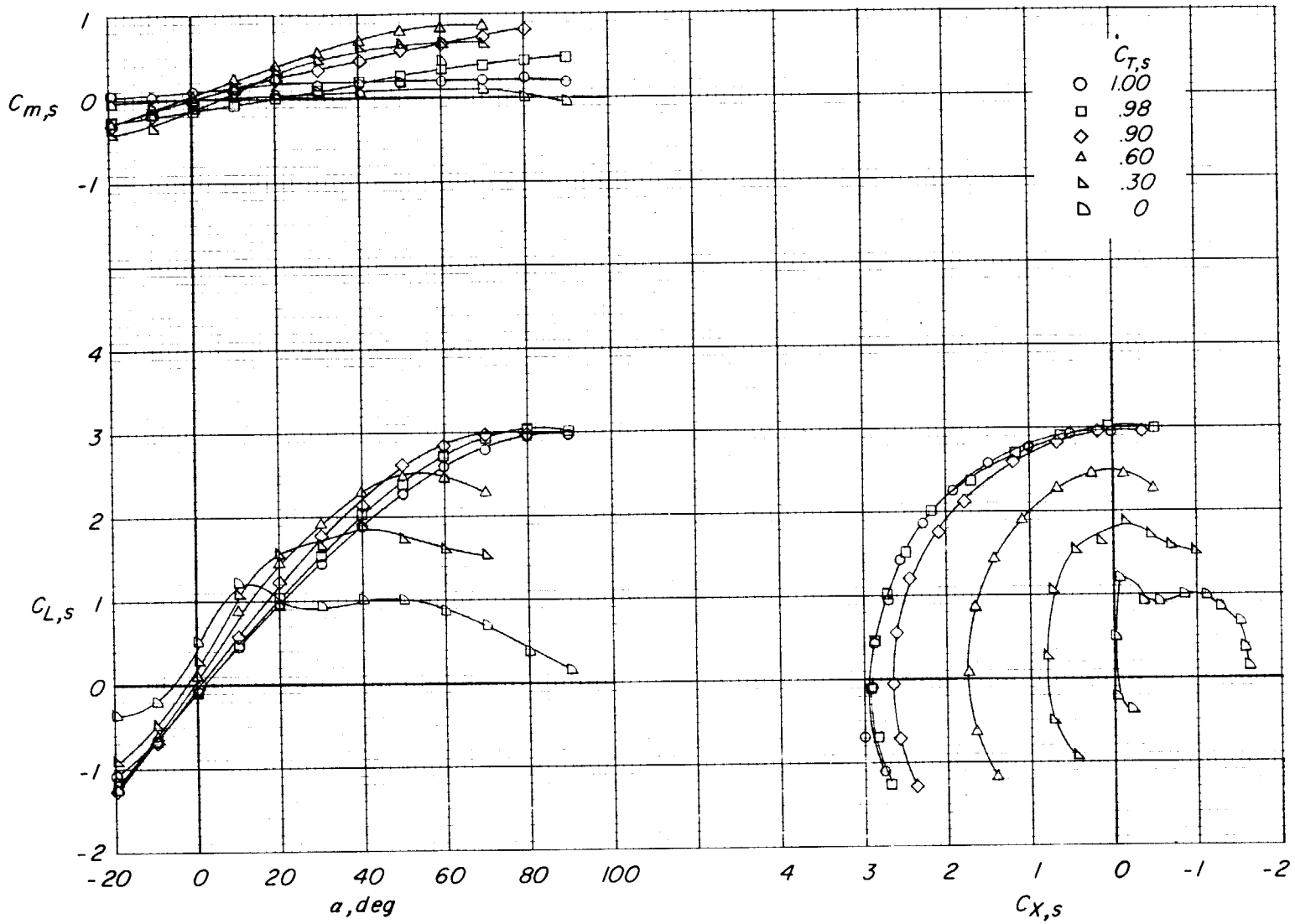

(a) $\delta_f = 0^\circ$.

Figure 7.- Aerodynamic characteristics of tilting-wing configuration with c/D = 0.333 and propeller rotation with wing-tip vortex. $i_p = 0^\circ$.

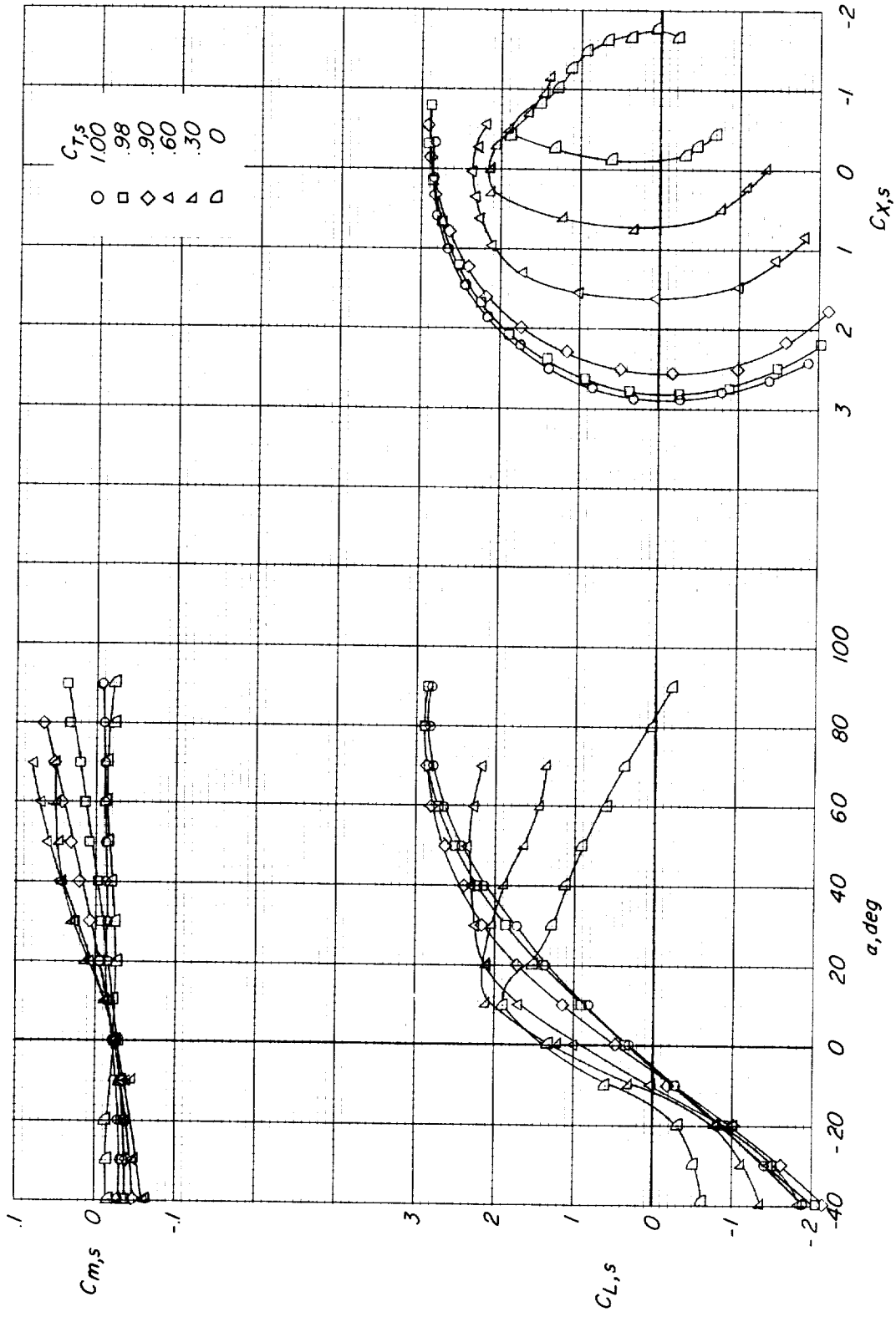

(b) $\delta_f = 50^\circ$.

Figure 7.- Concluded.

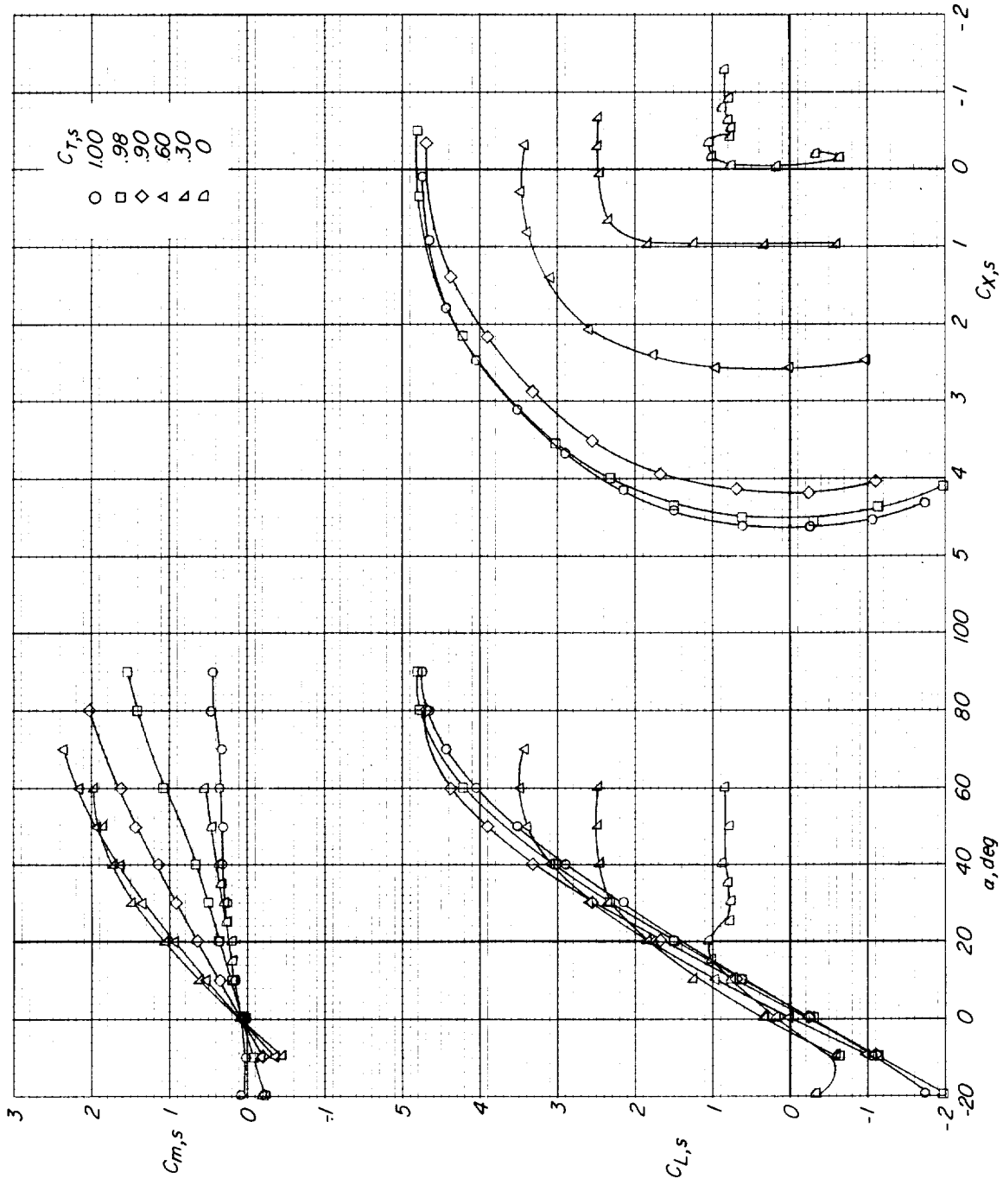

Figure 8.- Aerodynamic characteristics of tilting-wing configuration with c/D = 0.208 and propeller rotation with wing-tip vortex. $i_p = 0^\circ$; $\delta_f = 0^\circ$.

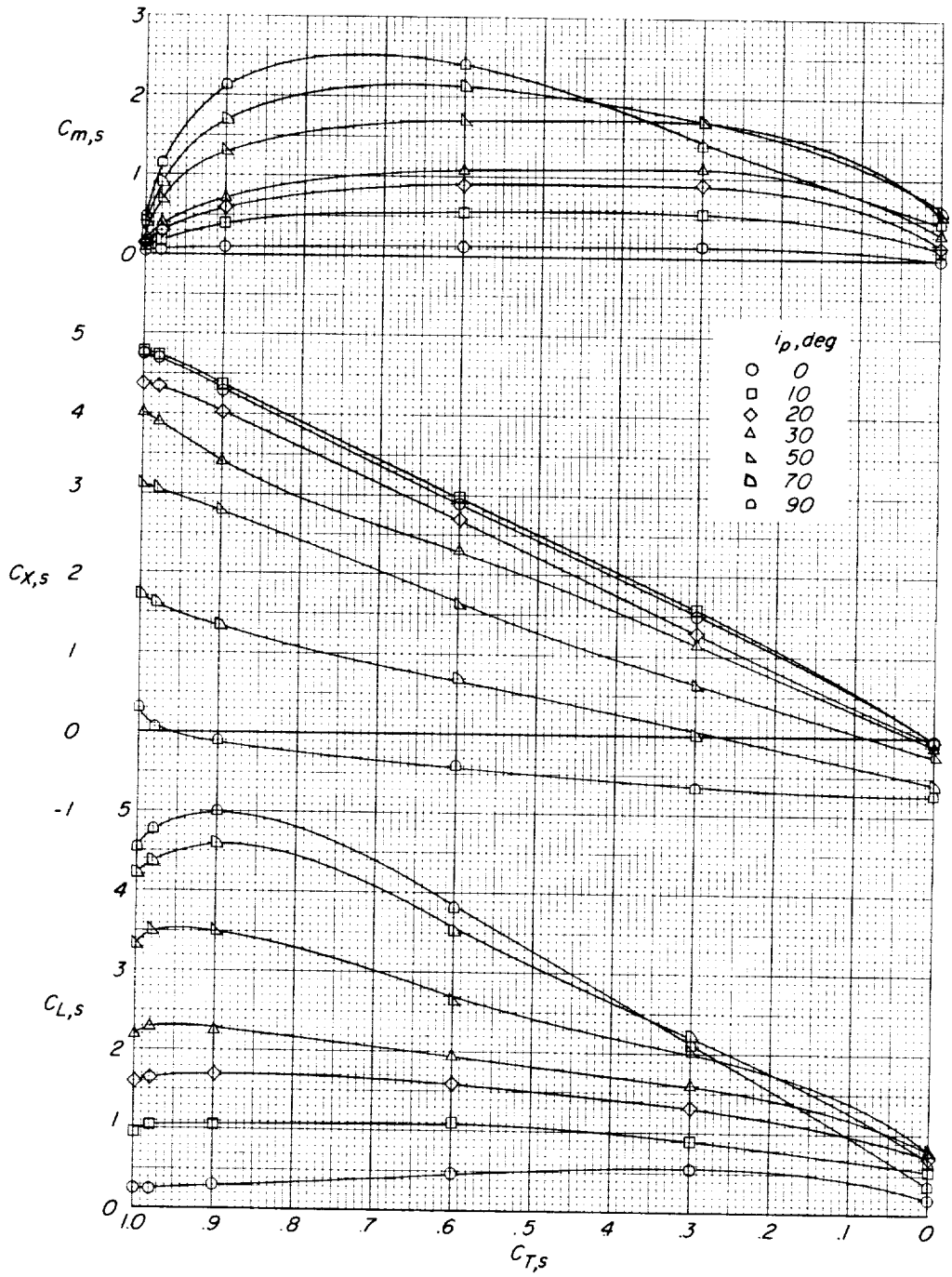

(a) $\alpha_w = 0^\circ$.

Figure 9.- Effect of change in propeller thrust-line incidence on the aerodynamic characteristics of the configuration with c/D = 0.208.

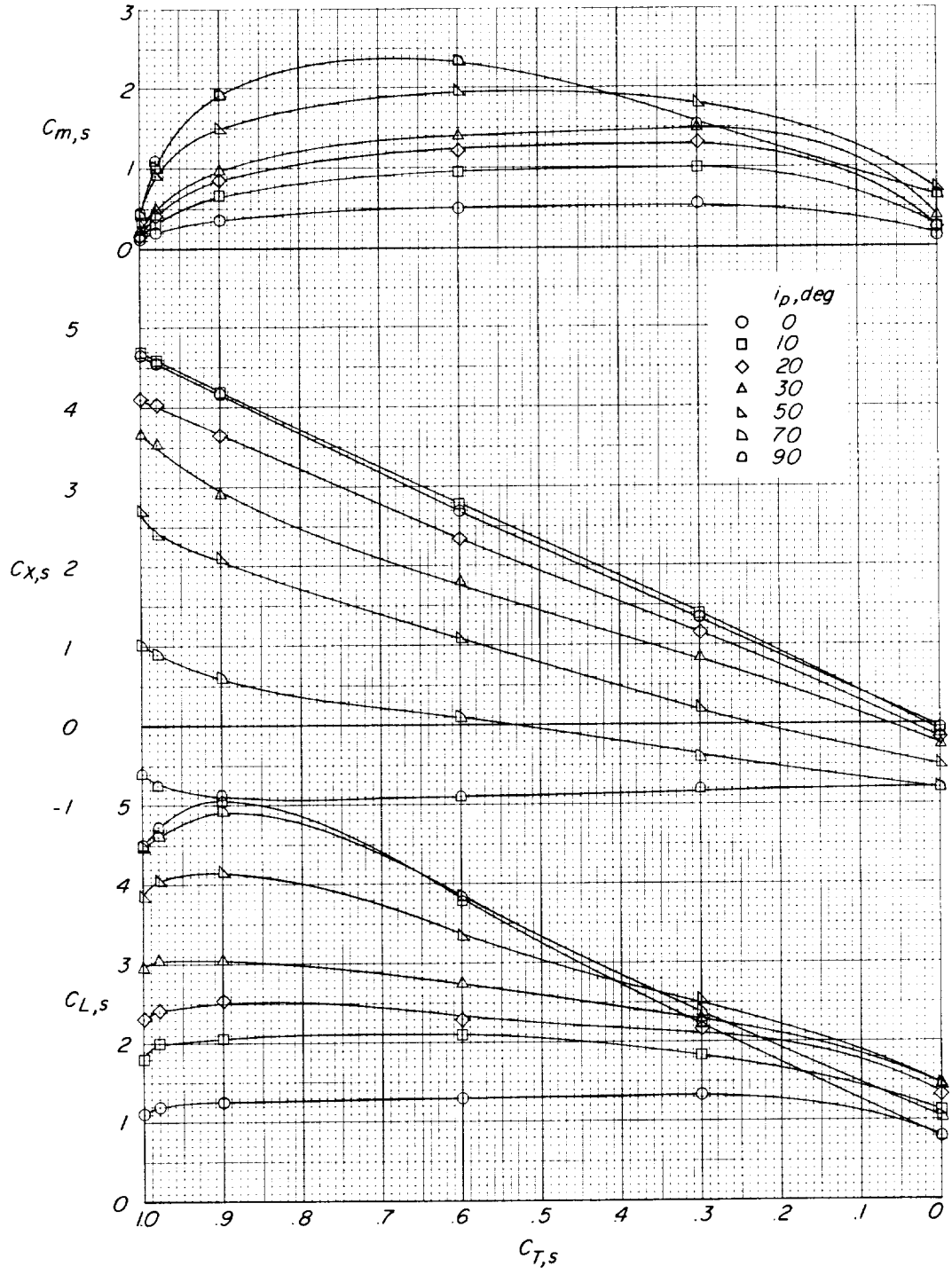

(b) $\alpha_w = 10^\circ$.

Figure 9.- Concluded.

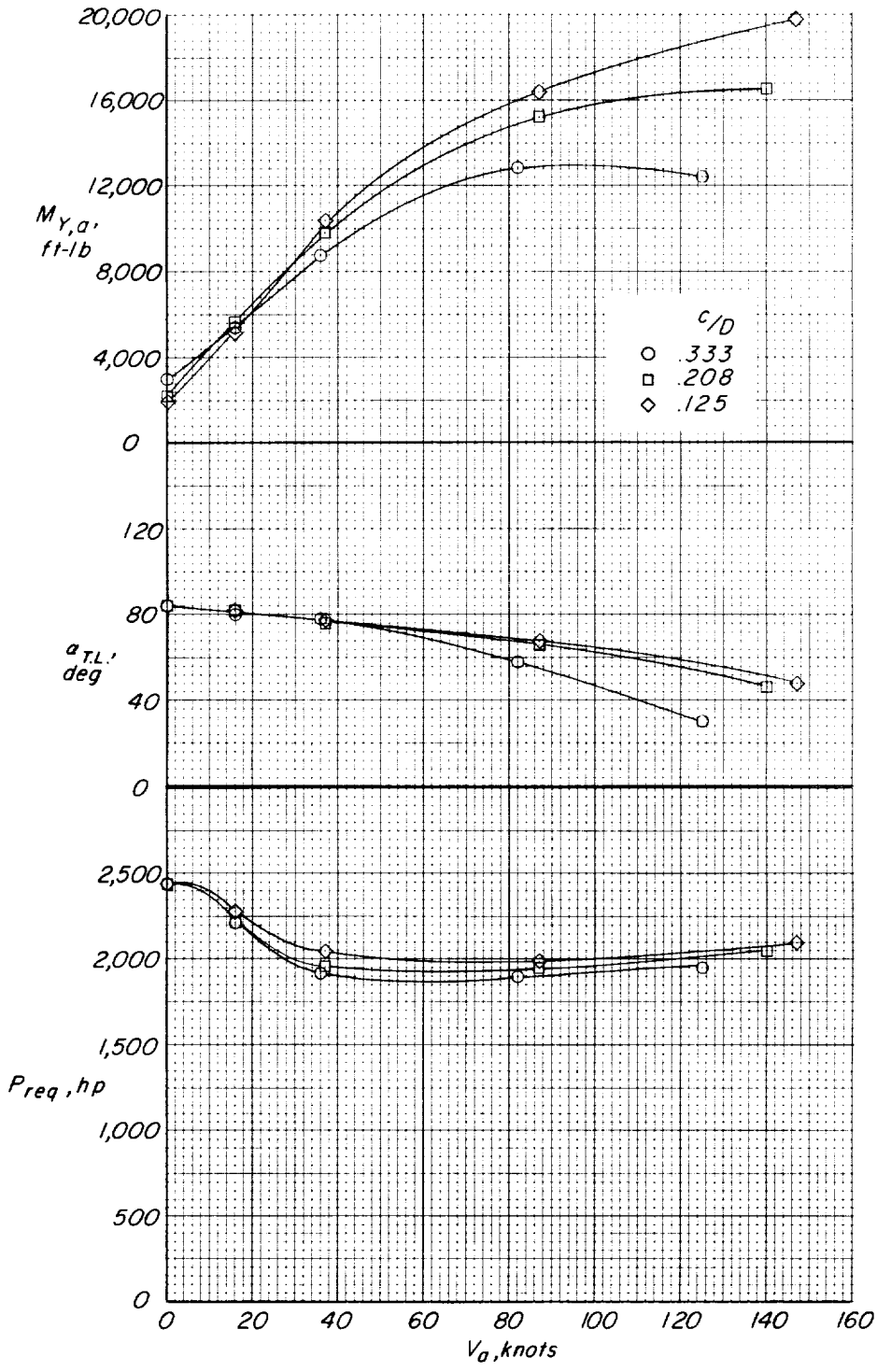

Figure 10.- Effects of changes in c/D on power required, thrust-line angle of attack, and pitching moment for an assumed 10,000-pound airplane in steady level flight.

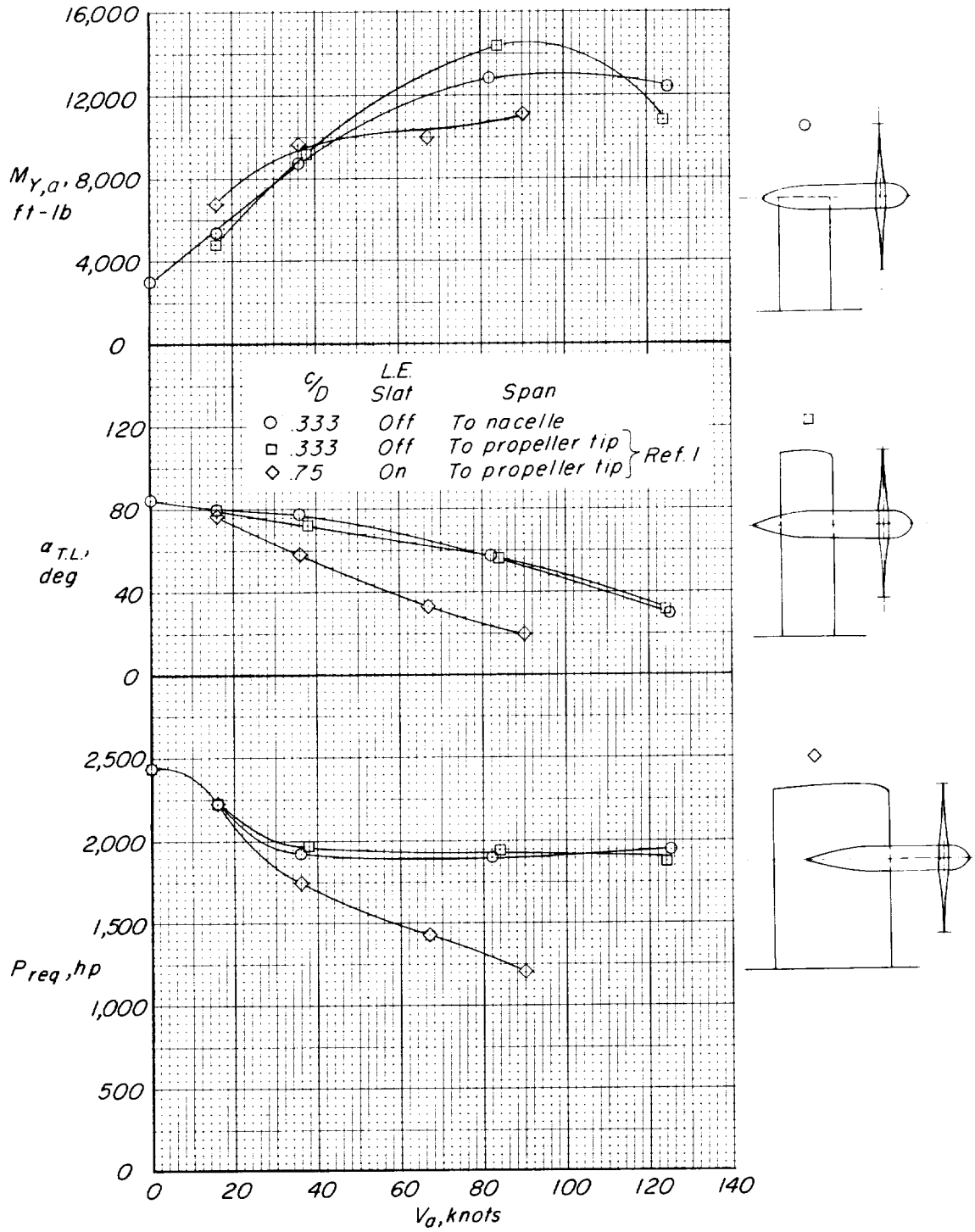

Figure 11.- Effects of c/D and wing span on power required, thrust-line angle of attack, and pitching moment for an assumed 10,000-pound airplane in steady level flight.

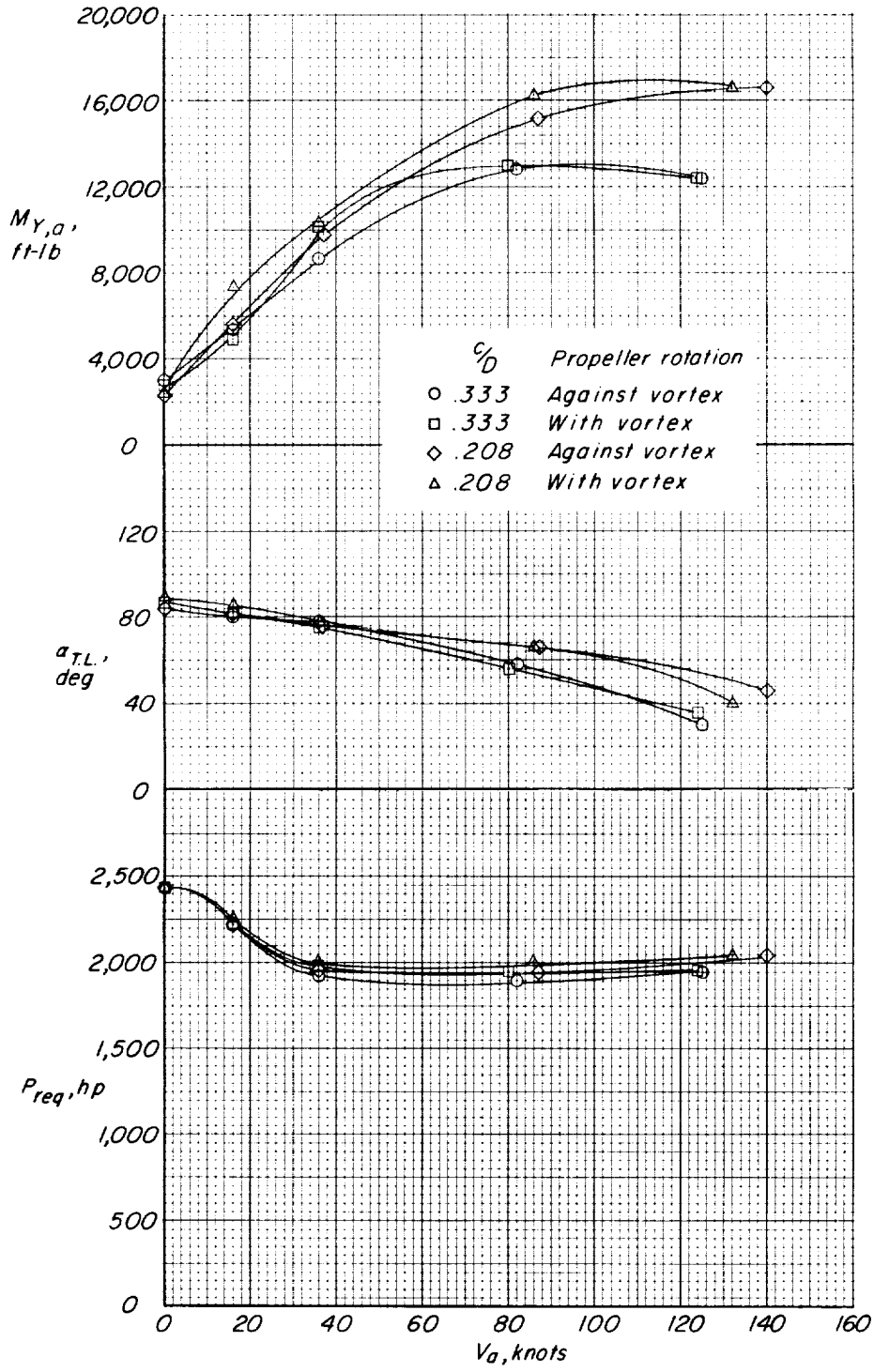

Figure 12.- Effects of propeller rotation on power required, thrust-line angle of attack, and pitching moment for an assumed 10,000-pound airplane in steady level flight.

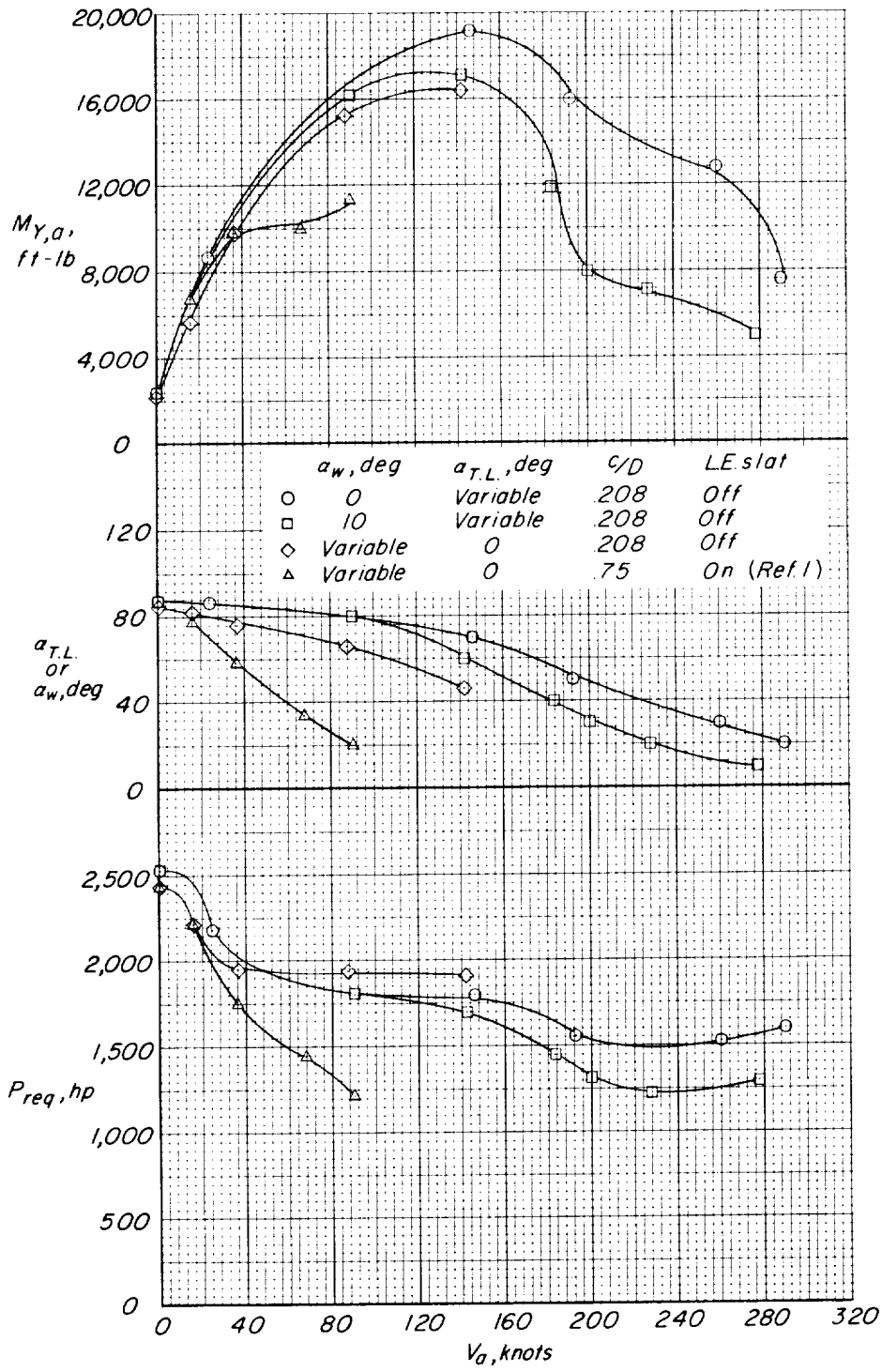

Figure 13.- Effects of wing angle of attack and propeller thrust-line incidence on power required and pitching moment for an assumed 10,000-pound airplane.